A MODEL FOR THE DISPERSION OF CONTAMINANTS IN THE SUBWAY ENVIRONMENT

L.R.Coke, J.G.Sanchez, and A.J.Policastro

Argonne National Laboratory

Synopsis

Although subway ventilation has been studied extensively, very little has been published on dispersion of contaminants in the subway environment. This paper presents a model that predicts dispersion of contaminants in a complex subway system. It accounts for the combined transient effects of train motion, station airflows, train car air exchange rates, and source release properties. Results are presented for a range of typical subway scenarios. The effects of train piston action and train car air exchange are discussed. The model could also be applied to analyse the environmental impact of hazardous materials releases such as chemical and biological agents.

1 INTRODUCTION

The need for a subway dispersion model has been discussed by Policastro et al. [1,2,3] in connection with analysis and mitigation of chemical/biological terrorist attacks on subways. Dispersion in a subway is a result of diffusion, exchange, and advection. Diffusion mainly occurs from mixing due to turbulence (eddy diffusion). Exchange occurs between the subway and exterior atmosphere at vents, entrances, portals, and also between train cars and subway tunnels and stations. Advection transports the contaminant predominately following the mean flow.

Dispersion predictions of a contaminant require knowledge of the velocity field. The problem is greatly simplified if the concentration prediction can be de-coupled from the solution for velocity. Such is the case for aerosols or gases that have little or no impact on the velocity field due to buoyancy or other effects. In such a case, the contaminant is characterised as a *passive scalar*. Most chemical and biological agents released in a subway airflow are expected to disperse as passive scalars. Consequently, the dispersion model presented in this paper functions as a post-processor that uses an independently derived velocity field.

The Subway Environment Simulation (SES) Model [4,5] is an established subway flow model that addresses many complex aspects of subway dynamics. Although it does not treat dispersion, it does predict the bulk mean velocities within tunnels, shafts, and stations. Subway flows are driven mainly by piston action of moving trains and fans, and, to a lesser degree, by natural buoyancy. A full solution by methods of computational fluid dynamics is infeasible for typical subways due to their

DISCLAIMER

large size and the high flow speeds generated by train motion. Alternatively, SES only solves for the *bulk mean flow* within a discrete set of finite subway elements under the assumption that the flow is incompressible. The mechanical energy equation (also known as the Bernoulli equation with losses) is applied to each control volume, or sub-segment, in SES terminology. The resulting system of linear equations is then solved as a Kirchhoff flow network. SES is a 1-dimensional (1-D) integral flow model. Despite its modest capability for flow prediction, the method is efficient, and even rigorous to the degree that the head losses within each sub-segment can be determined from similarity principles [4].

The new dispersion model, ANL/CB, was designed to be compatible with SES to the extent that it uses the 1-D subway segment concept. The SES Version 4.0 code was only modified to write its time-dependent velocity predictions in each subway sub-segment at selected internal time steps to a disk file. In this way, the velocity predictions could be easily accessed by the post-processing dispersion code. The SES internal time step for updating aerodynamics can be as small as one-hundredth of a second. ANL modified the SES code only to write essential data to a file at every internal SES step, or any multiple thereof. The data passed from the SES code to the ANL/CB code via this file includes the sub-segment geometry, the aerodynamic data of each sub-segment at each selected time step, and the train nose co-ordinates for each operating train on each route. The SES model required no change beyond the addition of extended file output.

2 FORMULATION OF DISPERSION MODEL IN SUBWAY NETWORK

2.1 Mathematical Basis

The transport of a scalar concentration $\Gamma(x_j,t)$, in a turbulent flow of an incompressible fluid, in tensor notation, is given by [8]:

$$\frac{\partial \Gamma}{\partial t}+\frac{\partial (U_j\Gamma)}{\partial x_j}=\frac{\partial}{\partial x_j}\left(\mathrm{T}\frac{\partial \Gamma}{\partial x_j}\right)+F_\gamma \qquad (1)$$

where T denotes the molecular transport coefficient and F_γ a source or sink term. To express equation (1) in terms of the mean quantities, introduce $\Gamma=\overline{\Gamma}+\gamma$, $U_j=\overline{U_j}+u_j$, to obtain

$$\frac{\partial \overline{\Gamma}}{\partial t}+\frac{\partial (\overline{U_j}\overline{\Gamma})}{\partial x_j}=\frac{\partial}{\partial x_j}\left(\mathrm{T}\frac{\partial \overline{\Gamma}}{\partial x_j}-\overline{U_j\gamma}\right)+F_\gamma \qquad (2)$$

The term $\overline{u_j\gamma}$ represents the effect of turbulent diffusion, which is typically much greater than molecular diffusion. The dominant mechanism for dispersion in a subway flow, by far, is advection. In some subways, trains may reach speeds approaching 100 kilometres per hour, thus generating a powerful piston action. Since the goal of this paper is to elucidate the predominant features of subway dispersion, neither molecular nor turbulent diffusion was included in the model at this time. Under these restrictions, the transport equation becomes

$$\frac{\partial \overline{\Gamma}}{\partial t} + \frac{\partial}{\partial x_j}\left(\overline{U_j}\overline{\Gamma}\right) = F_\gamma \tag{3}$$

For this study, the velocity field from SES was substituted for $\overline{U_j}$ as known data in equation (3); each segment interval was then solved piecewise for $\overline{\Gamma}$ subject to a given source term and prescribed boundary conditions. In SES terminology [5], a *segment* is a 1-D length of subway tunnel or shaft which has the same volumetric flow rate; *sub-segments* further divide a segment into lengths having the same cross-sectional area and thus a unique flow velocity. Conceptually, SES sub-segments are aerodynamic-equivalent control volumes, which join to form a Kirchhoff network of the subway (see Figure 1). Consider a network of sub-segments $k = 1,2,\ldots, N_s$ having lengths L_k, cross-sectional areas A_k, and mean velocity V_k. Applying equation (3) to each 1-D sub-segment k gives

$$\frac{\partial \rho(x,t)}{\partial t} + \frac{\partial}{\partial x}\left(V_k(t)\rho(x,t)\right) = F_k(x,t) \qquad k = 1,2,\ldots,N_s \tag{4}$$

where x is a local co-ordinate within the sub-segment and $\overline{\Gamma}$ has been replaced by ρ for notational convenience. Since $V_k^n(t)$ is independent of x, the above can be re-written as

$$\frac{\partial \rho(x,t)}{\partial t} + V_k(t)\frac{\partial \rho(x,t)}{\partial x} = F_k(x,t) \qquad k = 1,2,\ldots,N_s \tag{5}$$

which has the *hyperbolic character of a first-order wave equation* [9]. Appendix A contains a discussion of the finite difference scheme used in the ANL/CB code to solve equation (5).

2.2 Treatment of Sources

Sources for subway dispersion could be at locations such as on a station platform, inside a vent shaft, or inside a train car. A highly localised source can be modelled a *point source*. Sources having significant size and shape can be modelled as a collection of point sources. The ANL/CB model supports multiple point sources in combinations that suffice for modelling general releases. We will discuss the case of a single point source here; the generalisation to multiple sources is straightforward.

The term $F_k(x,t)$ in equation (4) represents the *source strength*; i.e., the contaminant mass per unit time that is added to the flow. It must be included in the finite difference equations for those sub-segments that contain a source. Appendix B discusses in some detail how point sources are included in the ANL/CB model.

Train cars, once infiltrated, become moving sources as they expel contaminant out from the car into the surrounding subway. A further complication is that cars may also behave as a sink, removing contaminant from the subway as it fills the car. The size of a car is significant, so it cannot be properly

modelled as a single point source. For these reasons, an independent sub-model was developed to address the complex nature of train car sources.

3 THE TRAIN CAR SUB-MODEL

Train cars have unique importance in subway dispersion because, once infiltrated, they become moving sources that transport concentration as fast as the cars move. The first arrival of contaminants at remote locations from the source is dictated by the speed of the trains rather than the usual dispersion mechanisms. Contaminated cars discharge relatively large amounts at scheduled stops since the source is momentarily stationary. Smaller amounts are discharged while the trains are moving throughout every subway section they pass through. In turn, the discharge continues to disperse by the usual mechanisms.

Train cars exchange air with the surrounding subway in three basic ways, as illustrated in Figure 2:

1. through intake to heating, ventilation, and air-conditioning (HVAC) systems inside the train cars,
2. through exchange when doors are opened at scheduled stops, and,
3. through leakage into the subway environment through cracks and other openings in the train car structure.

These mechanisms and the modelling of them are discussed below in subsequent sub-sections.

3.1 Contaminant Spread due to the HVAC System

The typical HVAC system draws air into vents at the top of the car. The dispersion model allows a constant HVAC fresh air intake rate to be specified. Since the flow is assumed incompressible, air from the car must be expelled at the same rate. The concentration of the inflow air depends on the subway concentration surrounding the car at any given instant. SES tracks the nose position of each operating train. That information is passed to the dispersion model, which then computes the grid location of each car for each operating train. At any instant, the HVAC exchange for a particular car occurs between the car interior and those sub-segment grid cells adjacent to the car (see Figure 3). It should be noted that the train car routine follows the concentration in each train car separately from other train cars. In addition, releases from the cracks of one train car as it moves becomes the source for contaminant for the next car and subsequent cars following that one. The specific treatment in ANL/CB of the train car source and uptake terms is given in Appendix C.

It should be noted that most train cars also recirculate the air that is in each car in addition to the separate intake and discharge of fresh air. This recirculation only helps to fully mix the car and does not add any dilution, so recirculation is not treated in the model. If the train car model actually predicted the concentration distribution in each car, then the recirculated amount would be important in predicting that distribution.

3.2 Exchange from Open Train Car Doors

The exchange through open car doors at scheduled stops is important to the model because it can significantly affect the concentration in the car and at the adjacent platform. The estimation of air exchange through doors has received attention because of its relevance to HVAC thermodynamics [4,15]. Two alternative methods are commonly employed to estimate the flow rate through an open car door. The first method is based upon the number of passengers that enter or exit through the door. Each passenger displaces a volume equal to that of his own body. Additionally, the motion of walking pushes a volume roughly equal to the displacement volume. The standard rule is therefore to count twice the body volume per each passenger that passes through the door. A typical body volume, B, would be about 0.07 cubic meters. If N_P is the total number of passengers both entering and exiting through the door, B the average body volume per passenger, and t_d the duration of the exchange, then the volumetric flow rate Q_{door} is simply

$$Q_{door} = \frac{N_p B}{t_d} \tag{6}$$

An alternate method [16] is to use a nominal flow velocity of 100 feet per minute (0.5 meters per second) assuming half the door area for inflow, the other half for outflow.

The ANL/CB code reads a fixed value of Q_{door} for each door on each train car. The concentration exchange between the car and the subway grid cell adjacent to the door is treated similarly to the HVAC exchange except here only one cell, at index i, is needed for any given door. The cell concentration is updated by

$$\rho_i(t_{n+1}) = \rho_i(t_n) e^{-\Delta t Q_{door}/(A_k \Delta x)} + \rho_{car}(t_n)\left(1 - e^{-\Delta t Q_{door}/(A_k \Delta x)}\right) \tag{7}$$

The change in mean concentration inside the car due to door exchange during the discrete time step t_n to t_{n+1} is

$$\Delta \rho_{car} = -\sum_i \left(\rho_i(t_{n+1}) - \rho_i(t_n)\right) A_k \Delta x \Big/ V_{car} \tag{8}$$

3.3 Exchange due to Leakage from Cracks

Crack leakage is the most difficult aspect of train car modelling because it is dependent upon the train velocity and the pressure differentials that build up inside the car. The combined leakage from cracks around doors and windows can be as large as the HVAC inflow [4,15]. The ANL/CB model presently allows only a constant leakage rate that is simply incorporated into and is equal in value to the HVAC inflow rate. Validation and refinements to the ANL/CB train car model are a subject of continuing research. It should be noted that, although the train car has special intake louvers from which air is sucked into the train car, there is no discharge port in the train car for the expulsion of air. All air expelled from the car through the HVAC system is through cracks, typically around the doors.

The ANL/CB model assumes that the rate of fresh air intake to a train car is always equal to the rate of air flow exhausted from the fully mixed car. The fresh air intake may have contaminant concentrations due to previous plume spreading..

4 THE AEROSOL DEPOSITION SUB-MODEL

Most chemical/biological releases are expected to be in aerosol form. A deposition sub-model contained within the ANL/CB subway network model accounts for the loss of concentration due to:

1. gravitational settling of aerosols (droplets or particulate),
2. deposition or aerosols on surfaces due to turbulent forced convection,
3. deposition or aerosols on surfaces due to natural convection, and,
4. deposition of aerosols on surfaces due to thermophoresis representing the mechanism due to temperature differences between walls and passing air.

The loss of concentration due to deposition is accounted for at each time step at each subway sub-segment location. A complete discussion of deposition is beyond the scope of this paper. The present deposition model accounts for the processes listed assuming homogeneous turbulence in the sub-segment methods. The formulation was adapted from References 12, 13, and 14. Difficulties in applying the thermophoresis sub-model results from the lack of data on temperature of subway walls as compared to air temperature in the layer of air adjacent to the walls. Deposition can be significant for particle or droplet sizes close to 1 micron. Droplet evaporation and vapour deposition is not yet accounted for in the model. Deposition of aerosols in train cars is a secondary effect and is currently not included in the model.

5 THE ANL/CB COMPUTER CODE

The ANL/CB compute code was written in Fortran 77 for use in any computer environment supporting the language. The program memory requirements vary according to the array size needed to simulate the subway elements. The critical parameters can easily be adjusted, and the code recompiled to increase the size limits. The compiled ANL/CB code required approximately one megabyte of memory to simulate the multiple line sample subway with its 216 sub-segments. By comparison, the SES code required approximately eight megabytes. Five input files are used by the ANL/CB code:

1. The train car data file contains the train and car specifications such as route locations where trains stop, HVAC and door flow rates, door locations and areas.
2. The junction data file contains the connecting sub-segment numbers at every SES node. These data are used to compute the concentration flows at junctions.

3. The aerosol data file contains the physical properties including size distribution of the contaminant.

4. The sub-segment output control file allows a user to select those particular sub-segments whose concentrations should be saved at periodic time steps.

5. The SES data containing sub-segment velocities, train location and speed are read at each time step as the ANL/CB code marches forward in time.

Two output files are written by ANL/CB. The concentration data are written to a binary file at selected time steps for each selected sub-segment. A summary of the fluxes through junctions and concentration mass for each sub-segment is written to a text output file. The summary also shows the state of train cars and overall mass distribution.

A variety of Fortran 77 utilities have been developed to further analyse the ANL/CB output files. The utilities produce readable output compatible with many commercial graphics products. The type of plots commonly employed here include:

- plots of the SES velocity field in any chosen sub-segment as a function of time,
- plots of the concentration and exposure at any chosen location as a function of time,
- plots of the spatial distribution of concentration and exposure in any chosen sub-segment or contiguous length of sub-segments at any given instant,
- plots of the spatial distribution of deposition in any chosen sub-segment or contiguous path of sub-segments at any given instant,
- plots of the temporal and cumulative mass expelled from any vent as a function of time,
- plots of the cumulative mass distribution for each state (aerosol, deposition, etc.) as a function of time.

For chemical/biological applications, it is often important to know the *exposure level* [1,2] of subway patrons. The instantaneous concentration field is a poor measure of its physiological impact. The exposure level provides a measure of the cumulative impact to the human body over a given time period. Exposures for the plots described above are derived by either of two forms, (1) *time-integrated concentration* (TIC) and (2) *dosage*. The former suffices for the study examples discussed here. The TIC as a function of position and time, $\tau(x,t)$, and is formally defined by

$$\tau(x,t) = \int_{t_o}^{t} \rho\ (x,t')dt' \qquad (9)$$

where t_0 is a reference time and x a fixed spatial co-ordinate. The ANL/CB plot utilities evaluate TIC's using a discrete integral approximation to (9).

6 STUDY CASES

6.1 A Sample Subway System

A generic prototype subway was developed to test the performance of the ANL/CB model as a tool for evaluating the impact of chemical/biological attacks on subways [3]. That same prototype was used here to demonstrate the behaviour of concentration under various conditions typical to subways. A plan view of the prototype subway is shown in Figure 4. The system consists of a two-level centre station (labelled "C"), and 12 side-platform stations. Two lines were modelled, one from North to South (N-S), the other from East to West (E-W). Each line extended approximately 3.5 kilometres outward from the centre to connect three stations in each direction. The stations were labelled as C, 1N, 2N, 3N, 1S, 2S, 3S, 1E, 2E, 3E, 1W, 2W, and 3W. Each tunnel section had a relief shaft before and after each station, and one fan shaft between the two relief shafts. Most sections were two-track tunnels, except for portions of single-track divided tunnels neighbouring Station C.

This study assumes a released aerosol having the following physical properties:

- aerosol specific gravity = 1.2
- thermal conductivity = 0.6 watts/meter-Kelvin
- tunnel air temperature = 298.1° Kelvin; wall temperature 294.3° Kelvin
- 3 particle size bins -

  Bin#1: mass fraction 25%, particle diameter 3 microns

  Bin#2: mass fraction 60%, particle diameter 4 microns

  Bin#3: mass fraction 15%, particle diameter 5 microns

These properties are selected for illustrative purposes only; they are reasonable choices but are not meant to characterise any particular subway or aerosol.

6.2 Velocity and Concentration Field in a Single Track Tunnel

This example illustrates the relatively simple case of a release from a source located in a single-track divided tunnel when the airflow is unidirectional. Trains were operated on only the northbound route with a uniform headway of 3 minutes. Each train was programmed to make only one stop, at station 3S, so as to generate a smooth velocity pattern allowing the focus to be on a simple case for illustration purposes. The piston action, as predicted by an SES simulation, generated the periodic

airflow shown in Figure 5. The figure shows the flow velocity within sub-segment 104-104 of a single-track divided tunnel just South of Station C on the N-S line. Since a sub-segment, by definition, has uniform cross-sectional area, the bulk mean velocity of an incompressible flow is constant throughout. The velocity plot therefore represents the time-dependent field at any fixed point within that sub-segment. As expected, the maximum peaks occur simultaneously with each passing train.

Subsequently, the SES predictions were used in an ANL/CB simulation of a steady, continuous localised source in sub-segment 104-104 at a track co-ordinate of 3200 meters on the N-S line. We assume that the initial concentration field is zero everywhere prior to the start of the release. According to equations (12) and (13), the local concentration should vary inversely with the local velocity. That expected behaviour is confirmed by the predictions illustrated in Figure 5.

The concentrations in this example continue to propagate beyond sub-segment 104-104 from the source towards the northbound direction. Each passing train generates a velocity "wave" that advances the extent of the concentration. Figure 6 shows the spatial distribution of the concentration field and exposures at a time of 1800 seconds after the start of release. The plot shows the instantaneous values of the two variables at each location along the track.

6.3 Velocity and Concentration Field for Bi-directional Train Motion

Bi-directional train motion in multiple track tunnels generates velocities of more complex form than that for unidirectional flow. The example considers the simultaneous operation of bi-directional trains on both lines in the system, two routes per line. Because the aerodynamics couple the air flows between the two lines through the interaction at the crossover Station C, the velocity profile shown in Figure 7 exhibits perturbations unseen in the previous example. .

The local concentration peaks appearing on either side of the source peak are caused by the discharge of concentration from train car doors at programmed stops in nearby stations. The source was located at mid-platform of Station C on the North-South line. Once the release starts, trains that stop at station C are heavily infiltrated. As those trains move to subsequent stations, the infiltrated cars discharge high concentrations while doors are open. This transport of concentration by cars adds a unique element to subway dispersion.

6.4 Velocity and Concentration Field in a Ventilation Shaft

Relief shafts, fan shafts, and station entrances all contribute to subway ventilation to at least some degree. The piston action of moving trains is often sufficient in itself to maintain adequate ventilation. This example assumes trains are running with fans off and dampers open. Then, all shafts that open to the atmosphere effectively act as ventilation shafts. The piston action of trains passing below a ventilation shaft generates a periodic, alternating velocity within the shaft (see Figure 10).

The concentration near the opening varies periodically with the flow reversal. The cycle is as follows:

1. As the nose of a train approaches the vent shaft, the increasing pressure pushes air up the shaft, expelling it into the atmosphere,

2. The train passes the vent shaft, and the pressure equalises,

3. After the rear of the train passes the vent shaft, the decreasing pressure pulls air down the shaft, drawing air from the atmosphere into the shaft.

The actual volume of fresh air exchanged depends upon the extent of the thrust within the shaft. If the shaft is very long, the net effect of the oscillation is merely to shift air between the tunnel and shaft. This might be the case for a long entrance passage to a station. On the other hand, if the shaft is relatively short the displacement likely exceeds the length of the vent shaft, so the oscillation completely flushes the shaft on both the upward and downward cycles. In that case, any concentration initially inside the shaft before the train arrives will be expelled, and then fresh air will be drawn down through the shaft into the tunnel.

Figure 11 shows the mass expelled from all of the ventilation shafts in the 2-line subway system, including fans shafts, relief shafts, and station entrances. The effect of each train can be seen in the peaks of the expelled flux plot.

6.5 The Overall Concentration Mass Distribution

At each time step, the ANL/CB computer code evaluates the total concentration mass distribution throughout the subway system, including

- the aerosol mass in each sub-segment,
- the mass deposited on the surfaces of each sub-segment,
- the aerosol mass in each train car, and,
- the aerosol mass that has escaped from each ventilation shaft or,
- a portal to the atmosphere.

Since the mass introduced into the subway by sources is also known, mass conservation can be verified (within numerical tolerance) throughout the simulation.

The distribution depends upon the subway design, the train and fan operations, and the source characteristics. Venting of aerosol to the atmosphere is enhanced by a high frequency of train motion. Obviously, exhaust fans expel concentration rapidly. The simulation described above for multiple line bi-directional train motion was run to produce the example shown in Figure 12. In this simulation, a single source was placed at mid-platform in station C. The source strength had a constant value of one gram per second for a duration of 5 minutes. The plot shows the rapid rise in aerosol during the initial release followed by a gradual decline due the venting and dilution caused by piston action.

Trains cars that stop to discharge passengers at Station C become infiltrated while the doors are open and, to a lesser degree, through the HVAC exchange. Once the doors close and the train moves away from the station, the HVAC exchange gradually flushes the cars. In this example the trains have a fixed headway of 3 minutes, so the process of loading and flushing at Station C leads to a quasi-

periodic variation in the total train car mass. The same process occurs for trains at other stops besides Station C, but the dominant effect of loading is at the source.

7 CONCLUSIONS

The ANL/CB is practical tool for predicting subway concentrations. It works in synchronisation with the SES subway flow model thereby accounting for the movement of multiple trains in tunnels and stations and accounting for the impact of blast and vent shafts. The dispersion model accounts for the intake and discharge of concentration from train cars as well as the movement of concentration due to the piston action of the trains. A first-order treatment of aerosol deposition is also included.

Exercise of the model in a generic subway case reveals the following features:

(a) the intake and discharge from train cars creates a rapid spread of contaminant to other stations and does so far faster than the piston effect,

(b) concentration history at a typical plume location where trains are routinely passing has a sinusoidal pattern which is about 180 degrees out of synchronisation from the sinusoidal pattern of the velocity field,

(c) Aerosol vented to the street increases with time when trains remain in operation during a release scenarios dominating the ultimate disposition of the mass as compared to the mass located in train cars, aerosols deposited in tunnels and stations, and aerosol remaining airborne in the tunnels and stations.

These conclusions are expected to be valid for other scenarios and represent the general nature of the contaminant dispersion in a subway system.

This effort is part of a continuing program at Argonne National Laboratory in support of the U.S. Department of Energy PROTECT Program. Efforts are in progress to further improve the ANL/CB model, and to validate it against test data.

8 ACKNOWLEDGEMENTS

The authors express their thanks to Scott R. Filer, DIS Division, Argonne National Laboratory, for his assistance in the editing and preparation of this manuscript.

References

[1] Policastro, A.J. and Coke, L. *Protecting U.S. Subway Systems from Chemical/Biological Terrorism.* Transit Policing, Vol. 8 No. 1, 1998.

[2] Policastro, A.J., L. Coke, G. Sanchez, D. Brown, and W. *Dunn Modeling Chemical/Biological Dispersion in Subways.* Presented at DOE Chemical/Biological Nonproliferation Program, Annual Meeting, Los Alamos National Laboratory, July 22, 1999.

[3] Sanchez, J.G., Coke, L.R., Wasmer, F.L., and Policastro, A.J. *Comparison of Strategies in Managing Chemical/Biological Releases in the Subway Environment.* Third International Conference, Tunnel Management 2000, Abstract approved for paper presentation, Sydney, Australia, 4-6 October, 2000.

[4] Parsons, Brinckerhoff, Quade, and Douglas, Inc. and ICF Kaiser Engineers, Inc. Subway Environmental Design Handbook, Volume I, *Principles and Applications*, 2nd Edition, Associated Engineers, National Technical Information Service No. PB-254-788, 1976

[5] Parsons, Brinckerhoff, Quade, and Douglas, Inc. and ICF Kaiser Engineers, Inc. Subway Environmental Design Handbook, Volume II, *Subway Environmental Simulation Computer Program - SES Version 4, Part I User's Manual*, Report No. FTA-MA-26-7022-97-1, prepared for U.S. Department of Transportation, Research and Special Programs Administration, Volpe National Transportation Systems Centre, Cambridge, Massachusetts, December 1997.

[6] Barton, G. *Elements of Green's Functions and Propagation.* Oxford University Press, Oxford, 1991.

[7] Crank, J. *The Mathematics of Diffusion.* Oxford University Press, Oxford, 1975.

[8] Hinze, J.O. *Turbulence* McGraw-Hill, Inc, New York, 2nd edition, 1975.

[9] Lighthill, M.J. Sir *Waves in Fluids.* Cambridge University Press, Cambridge, 1978.

[10] A.R. Mitchell and D.F. Griffiths. *The Finite Difference Method In Partial Differential Equations.* John Wiley and Sons, New York, 1980.

[11] Fletcher, C. A. J. *Computational Techniques for Fluid Dynamics*, Vols. I and II. Springer-Verlag, New York, 1988.

[12] Nazaroff, W. W. and Cass, G.R. *Particle Deposition from a Natural Convection Flow onto a Vertical Isothermal Plate*, Journal of Aerosol Science, 15, 567-584, 1987.

[13] Nazaroff, W. W. and Cass, G. R. *Mass Transport Aspects of Pollutant Removal at Indoor Surfaces*, Environment International, 15, 567-584, 1989.

[14] Petukhov, B. S., *Heat Transfer in Turbulent Pipe Flow*, Advances in Heat Transfer, 6, 503-564, 1970.

[15] New York City Transit Authority, *Part II of an Air Conditioning Study of the New York City Transit System, Feasibility of a Thermoelectric Air Conditioner for Subway Cars,* Prepared by Westinghouse Electric Corporation, Project NY-MTD-12, 1968.

[16] Developmental Sciences, Inc. Aerospace Technology Division, *Subway Aerodynamic and Thermodynamic Test(SAT) Facility—Single Track Thermodynamics*, City of Industry, 1972, Technical Report No. UMTA-DC-MTD-7-72-16.

Appendix A Finite Difference Formulation of ANL/CB Dispersion Model

To obtain a discrete equivalent of equation (5), each sub-segment k is divided into N_k equal intervals $\Delta x = L_k/N_k$ to form a spatial grid $[x_1, x_2, ..., x_{N_k}]$. The temporal grid is defined by a fixed stepsize, Δt, and corresponding time steps $t_n = n\Delta t$. We seek to find the cell-averaged mean value for ρ at time t_n,

$$\rho_i^n = \frac{1}{\Delta x}\int_{x_{i-1}}^{x_i} \rho(x, t_n)dx \qquad \text{(A-1)}$$

The natural finite difference interpretation suggests that ρ_i^n be placed at mid-cell in cell i. A second-order accurate finite difference formula in a sub-segment having no internal sources when $V_k(t) \geq 0$ is

$$\rho_i^{n+1} = \rho_i^n + r\left(\rho_{i-1}^{n+1} - \rho_i^{n+1}\right) + r\left(\rho_{i-1}^n - \rho_i^n\right) \quad i = 1,2,...,N_k \qquad \text{(A-2)}$$

where $r = V_k\Delta t / \Delta x$. Similar finite difference forms are well established in connection with the wave equation and the *upwind* treatment of the 1-D convection term [10,11]. The cell-centred concentrations at indices $[i-1, i]$ are appropriate for flow in the *upwind direction* (in the sense of increasing i). For $V_k(t) \leq 0$, the corresponding formula for flow in the *downwind direction* is:

$$\rho_i^{n+1} = \rho_i^n + r\left(\rho_i^{n+1} - \rho_{i+1}^{n+1}\right) + r\left(\rho_i^n - \rho_{i+1}^n\right) \quad i = 1,2,...,N_k \qquad \text{(A-3)}$$

The boundary conditions for equations (A-2) and (A-3) are determined by the inflows/outflows at sub-segment junctions to assign ρ_0^{n+1} or ρ_{Nk+1}^{n+1}. At simple SES junctions, the boundary conditions are the concentrations at the adjacent endpoint of the upwind sub-segment that feeds the junction. At portals and vents to the atmosphere, the inflow boundary condition is just the ambient concentration, usually zero. The corresponding outflow boundary condition acts as a sink.

At multiple junctions, the boundary conditions require special treatment. SES allows up to five sub-segments per junction. The flow directions in each sub-segment are time-dependent, so many combinations are possible. For a junction at the downwind end of a sub-segment, the outflow simply acts as sink. At an inflow junction, the boundary condition for the upwind end of the sub-segment is determined by flux-weighted mixing using

$$\rho_b = \frac{\sum_{all\ inflows} \rho_i Q_i}{\sum_{all\ outflows} Q_k} \qquad \text{(A-4)}$$

For multiple junctions of three or fewer sub-segments, equation (A-4) is rigorous. However, when

applied to more than three junctions, it entails the additional assumption that all inflows are *fully mixed* in the stream at the point of the junction.

Although implicit in appearance, equations (A-2) and (A-3) can be solved explicitly by a simple marching scheme. To illustrate, re-write equation (A-2) in the form

$$\rho_i^{n+1} = \frac{\left(\rho_i^n - r\,\rho_i^n + r\,\rho_{i-1}^n + r\,\rho_{i-1}^{n+1}\right)}{(1+r)} \qquad i = 1,2,\ldots,N_k \tag{A-5}$$

The right hand side of equation (A-5) is explicit provided that the ρ_{i-1}^{n+1} are updated sequentially, starting with the known boundary point , where

$$\rho_0^n = \rho_b^n, \quad \rho_0^{n+1} = \rho_b^{n+1} \tag{A-6}$$

For flow in the downwind direction of a sub-segment, an explicit solution of (A-3) is obtained similarly, except that the marching proceeds from the known boundary condition from (A-4) to set ρ_{Nk+1}^n and ρ_{Nk+1}^{n+1} at $i = N_k + 1$, with i decreasing. In either case, the solution is numerically stable provided the Courant-Friedrichs-Levy condition [11], $r \le 1$, is satisfied. [Although the discrete equations here resemble the unconditionally stable Crank-Nicolson form, the important difference is that, here, r is time-dependent.

Appendix B Accounting for Source Terms in ANL/CB Model

Since the grid spacing Δx limits the resolution, combinations of localised point sources are the most general that can be adapted in this model. Consider a source located in cell i of sub-segment k (see Figure 1). The cell volume is $\Delta x A_k$. During a time-step Δt, the source $F_k(x_i,t)$ adds a mass $\Delta t F_k(x_i,t)$. The incremental change in the cell mean concentration is given by

$$\Delta\rho_i^n = \frac{\Delta t\, F_k(x_i,t_n)}{\Delta x\, A_k} \tag{B-1}$$

A term corresponding to the right side of equation (B-1) is incorporated in the ANL/CB model for each point source. Its accuracy can be tested by comparing the discrete term to its theoretical value in the continuum case. The source $F_k(x_i,t)$ releases a mass $\Delta t F_k(x_i,t)$ during the interval Δt to the control volume $AkVk\Delta t$. In the limit at $\Delta t \to 0$, the local mean concentration is

$$\rho(x_i,t_n) = \frac{F_k(x_i,t_i)}{A_k V_k} \tag{B-2}$$

Note that equation (B-2) is instantaneously exact, whereas equation (B-1) must be integrated over a series of time steps in order to obtain the approximate local concentration.

The propagation of concentration as governed by equation (5) is linear; its solutions are therefore subject to the well-known *superposition principle* [6,7]. [To be precise, the solution within each sub-segment is linear; the global solution is piece-wise linear] One immediate consequence of this property is that all points of the concentration field scale in direct proportion to the source strength. Without loss of generality, the source term in equation (B-2) can be written

$$F_k(x_i, t_n) = F_k^0 f(x_i, t_n) \tag{B-3}$$

where F_k^0 is a scaling constant and $f(x_i, t_n)$ an arbitrary function of position and time scaled so that its maximum value is unity. For a given fixed function, f, the effect of the factor F_k^0 is merely to multiply the source and concentration solution field everywhere by the same factor. Note, however, the fundamental time-dependence of the source must remain fixed.

Appendix C Finite Difference Treatment of Train car Source Terms

Presently, the train car model predicts only the mean concentration as a function of time, ρ_{car}, in each car. Let Q denote the HVAC fresh air intake flow rate, L_{car} the car length, and V_{car} its volume. The proportion of Q entering the car from a bounding cell i of length Δx is computed by

$$\Delta Q_i = \frac{Q\Delta x}{L_{car}} \tag{B-4}$$

The corresponding elemental volume flow rate is

$$\Delta Q_i \Delta t = \frac{Q\Delta t\Delta x}{L_{car}} \tag{B-5}$$

Since the flow is incompressible, an equal volume must be discharged from the train car back into each subway cell. The net concentration mass transfer from cell i into the car is therefore

$$\Delta m_i = \frac{Q\Delta t\Delta x}{L_{car}}(\rho_i - \rho_{car}) \tag{B-6}$$

The term Δm_i is positive when the subway contamination, ρ_i, exceeds that in the car; it is negative if the reverse is true.

Dividing equation (B-6) by the car volume gives the net change in the car concentration due to exchange with cell i :

$$\Delta \rho_{car_i} = \frac{Q \Delta t \Delta x}{L_{car} V_{car}} (\rho_i - \rho_{car}) \tag{B-7}$$

The corresponding change in concentration of cell i of sub-segment k is

$$\Delta \rho_i = -\frac{\Delta m_i}{A_k \Delta x} = \frac{Q \Delta t}{A_k L_{car}} (\rho_{car} - \rho_i) \tag{B-8}$$

In practice, indiscriminate use of equation (B-8) can lead to negative concentrations due to round-off error. Subsequently, the discrete equations may become unstable. Alternatively, consider the limiting continuum equation

$$\frac{\partial \rho_i}{\partial t} = \frac{Q}{A_k L_{car}} (\rho_{car}(t) - \rho_i(t)) \tag{B-9}$$

Equation (B-9) is generally intractable due to the complexity of $\rho_{car}(t)$. However, ρ_{car} is nearly constant over a single time step Δt. In that case, the analytical solution for the time step is

$$\rho_i(t_{n+1}) = \rho_i(t_n) e^{-\Delta t Q/(A_k L_{car})} + \rho_{car}(t_n)\left(1 - e^{-\Delta t Q/(A_k L_{car})}\right) \tag{B-10}$$

Equation (B-10) serves as a relaxation method that replaces (B-9) to eliminate the potential instability. Each cell bounding the car is updated using (B-10), then the total mass increase for all cells over the time step is computed by

$$\Delta m = \sum_i \Delta m_i = \sum_i (\rho_i(t_{n+1}) - \rho_i(t_n)) A_k \Delta x \tag{B-11}$$

By mass conservation, the corresponding change in the car must be $-\Delta m$. Therefore, the change in mean concentration inside the car due to HVAC exchange during the discrete time step, Δt, is

$$\Delta \rho_{car} = -\frac{\Delta m}{V_{car}} \tag{B-12}$$

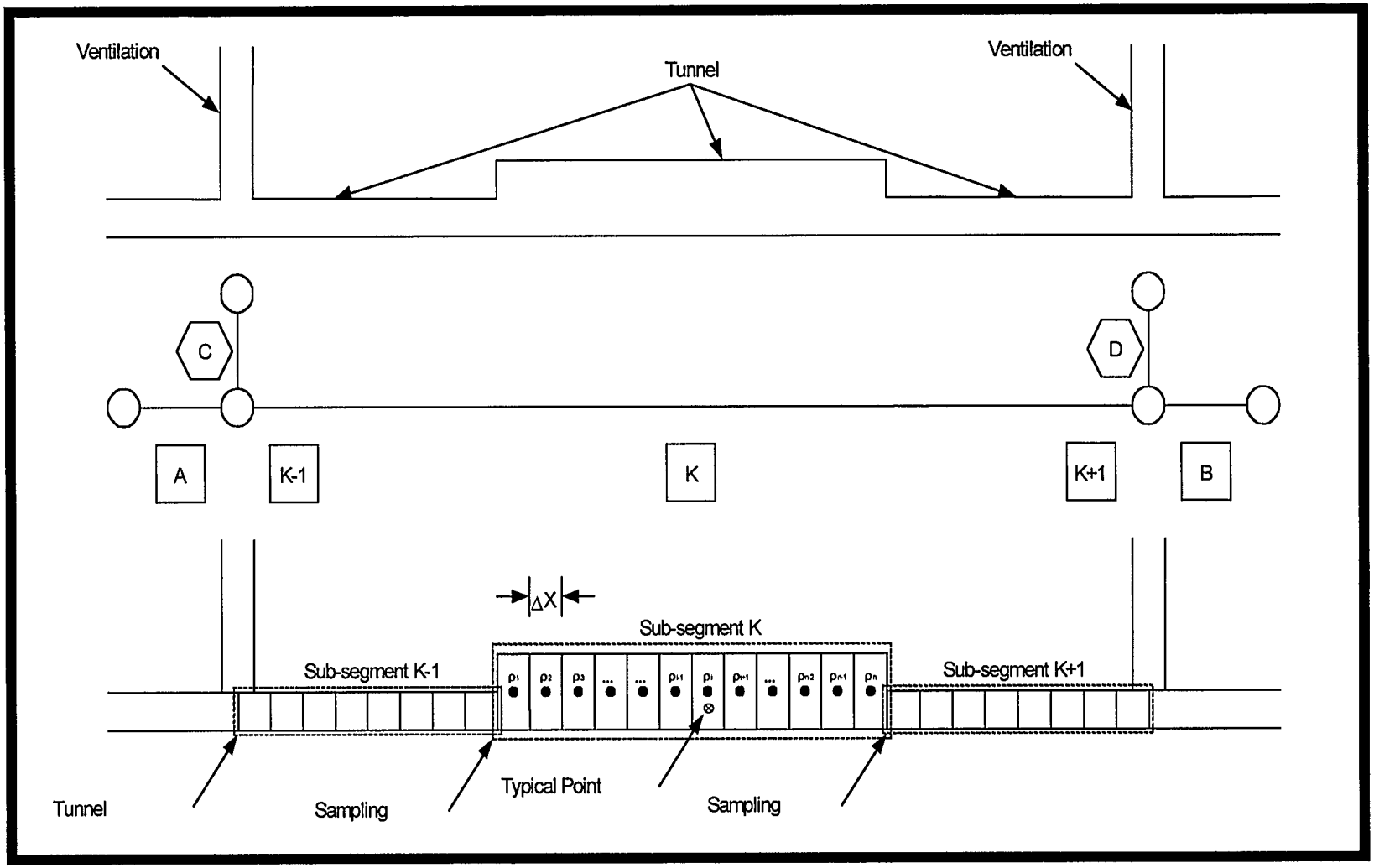

Figure 1: Typical SES Node Diagram

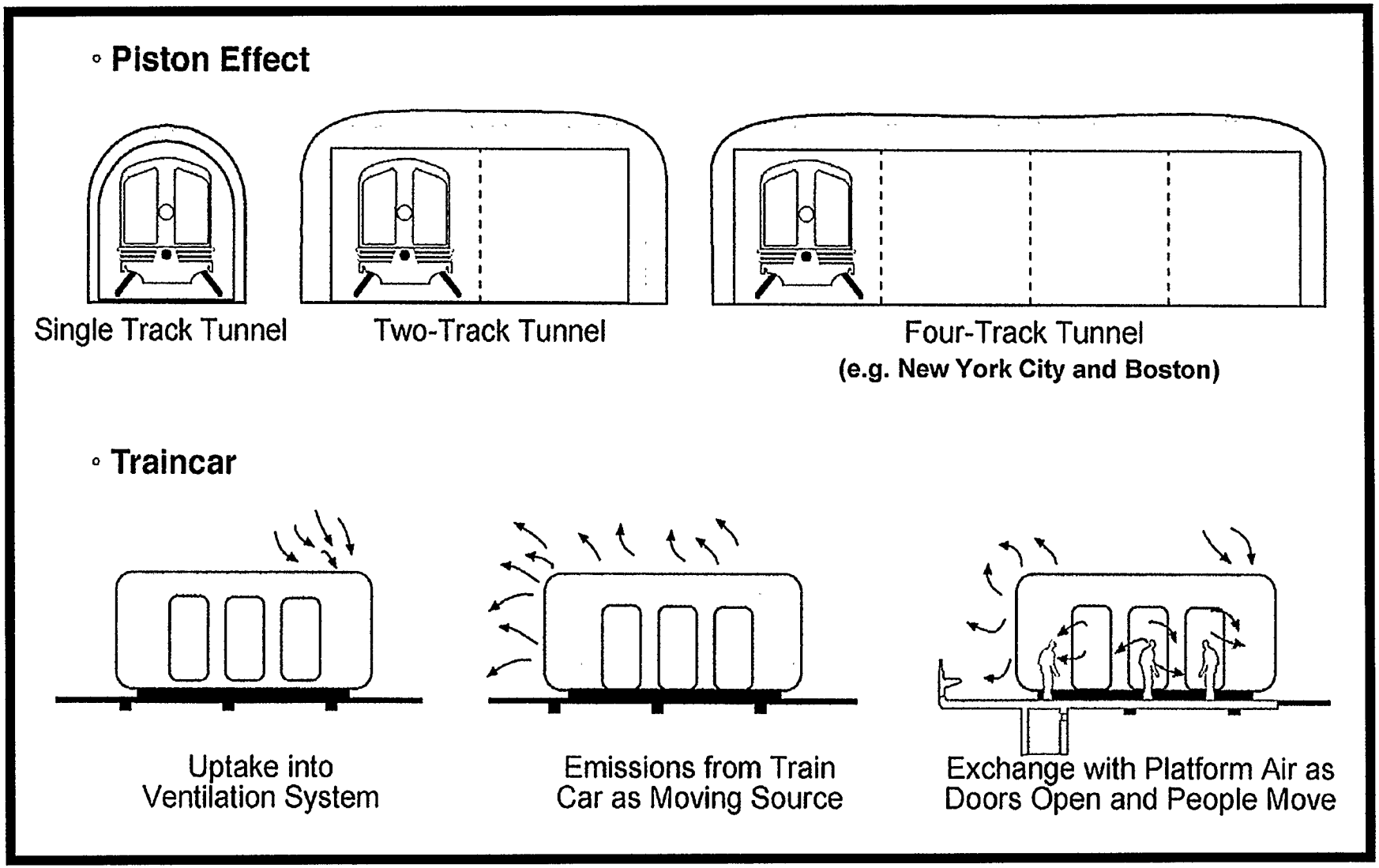

Figure 2: Schematic of Train Car Exchange Process

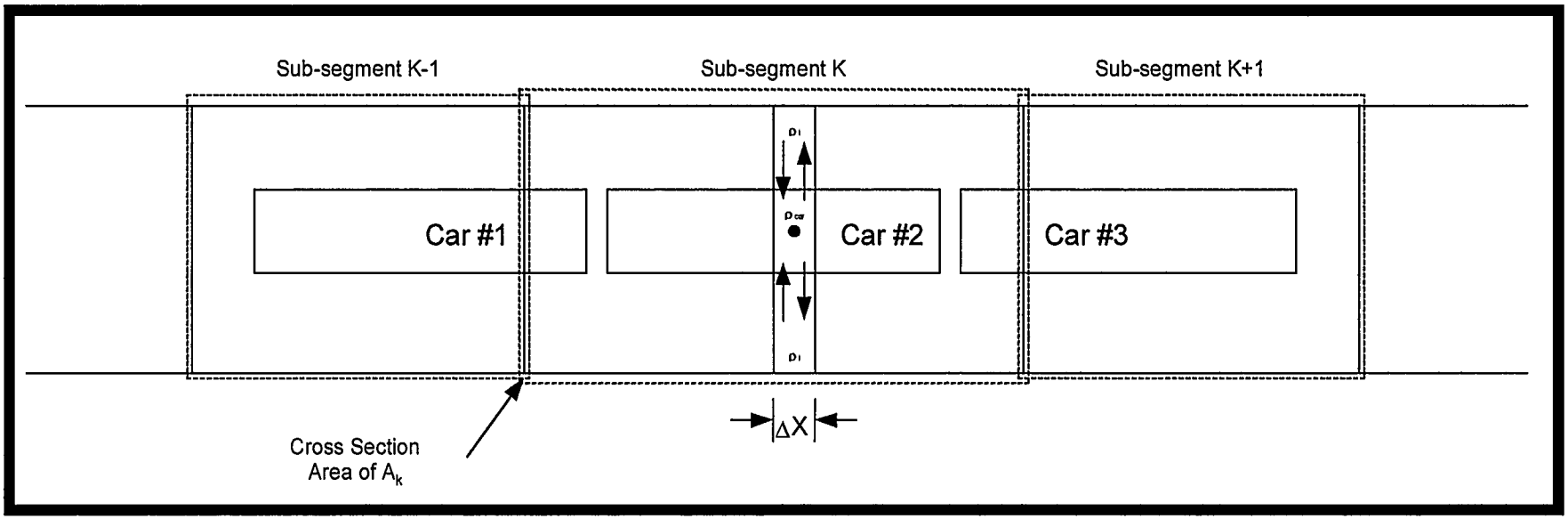

Figure 3: Control Volumes for Train Car HVAC Air Exchange Model

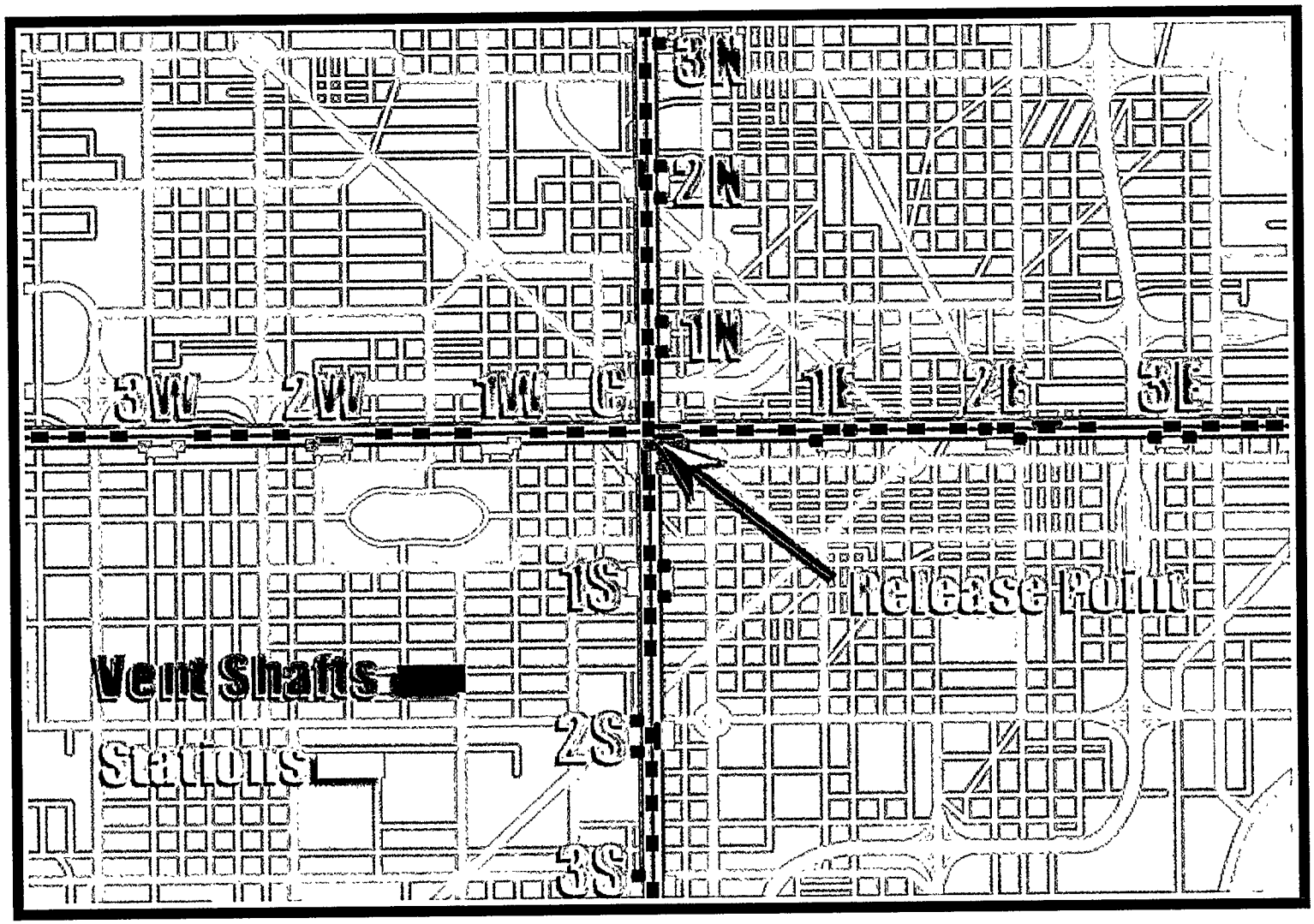

Figure 4: Prototype Subway System
North – South and East - West

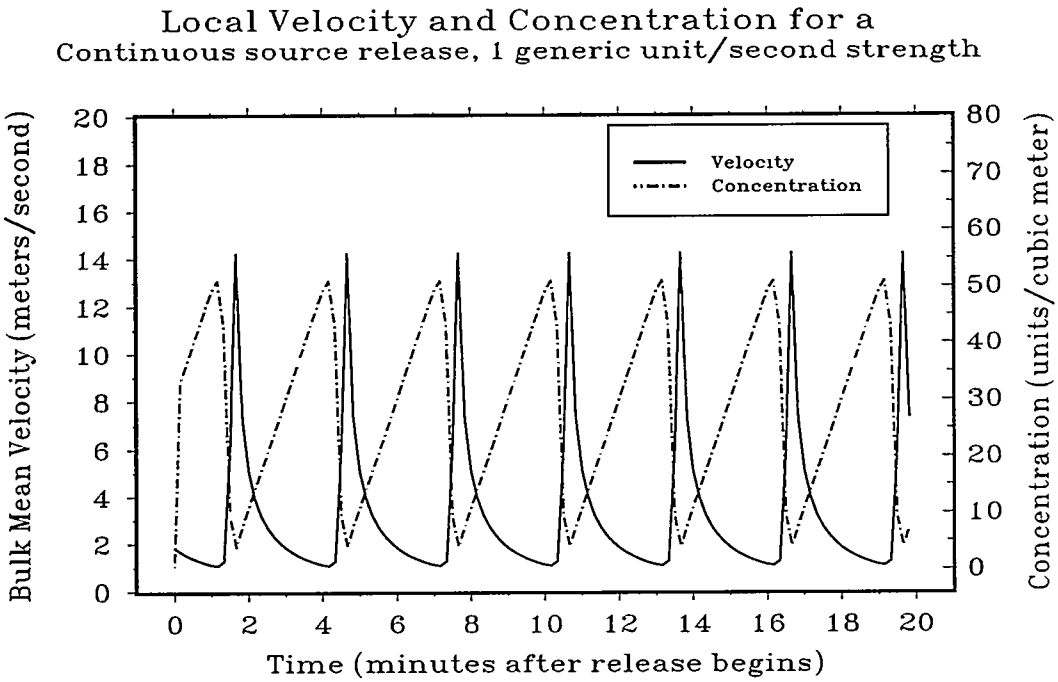

Figure 5: Local Velocity and Concentration over source

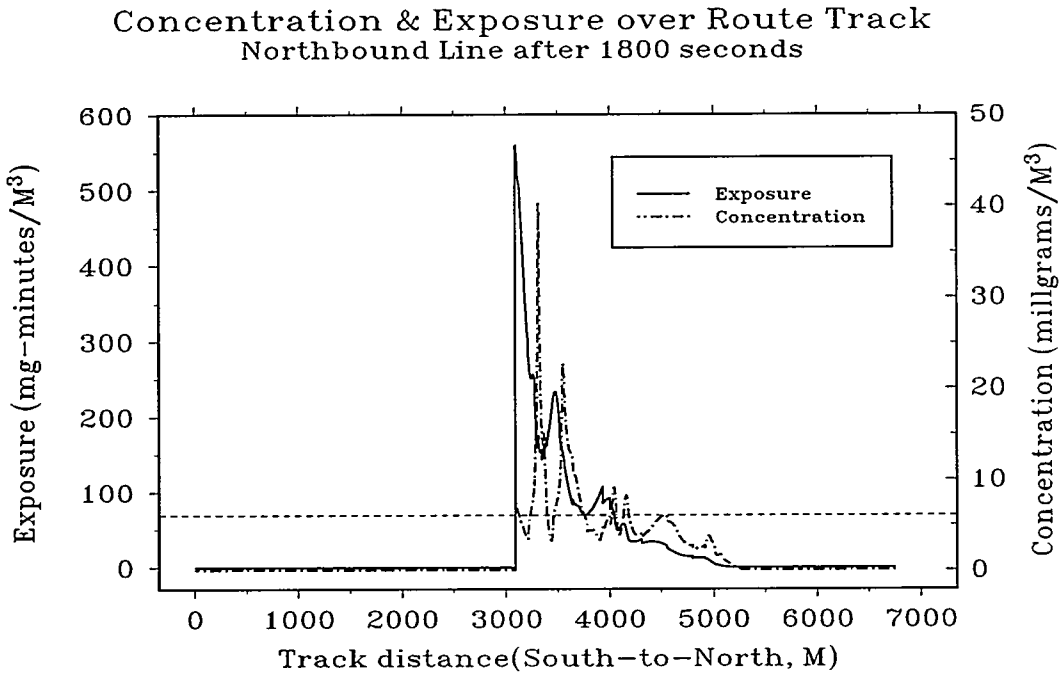

Figure 6: Example of Concentration and Exposure for 1-directional Train Motion

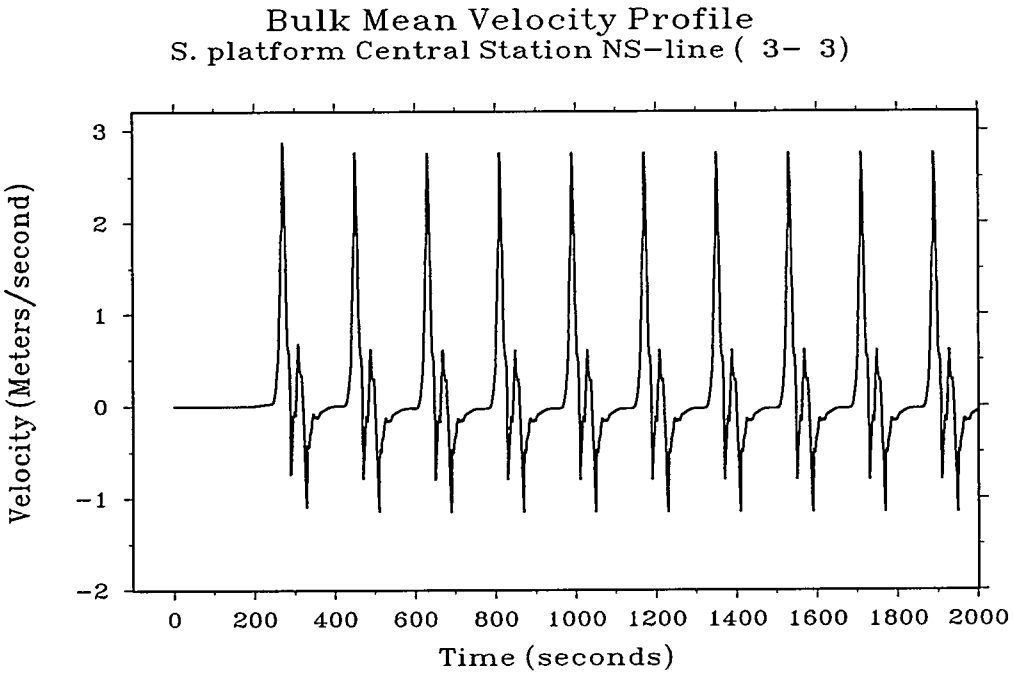

Figure 7: Velocity profile for Bi-directional Train Motion

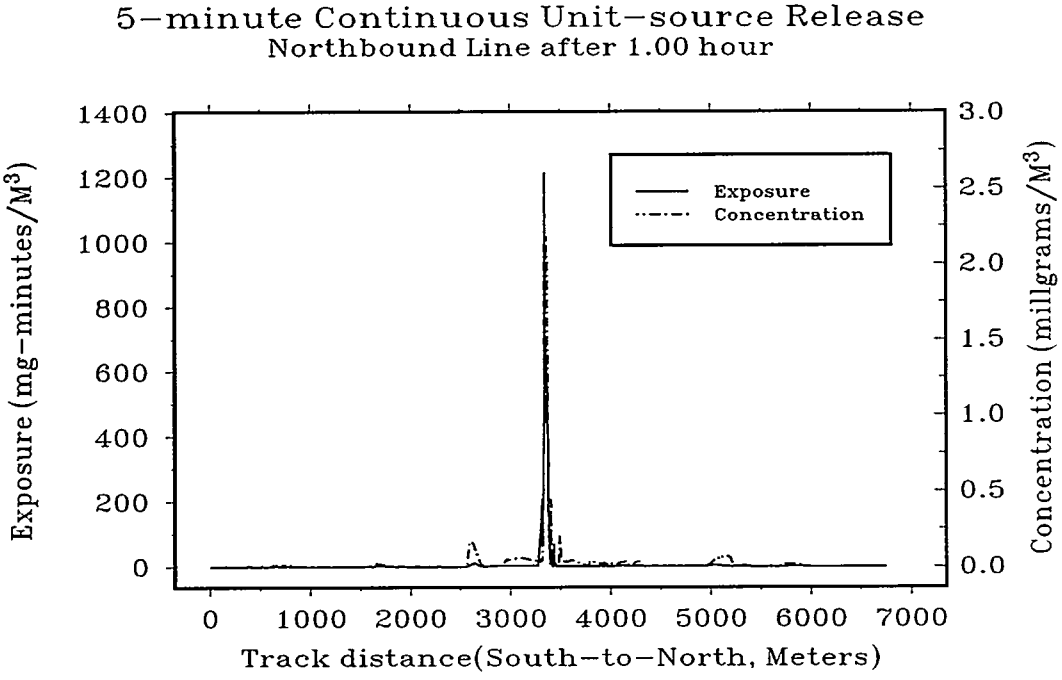

Figure 8: Concentration Field for Bi-directional Train Motion Example

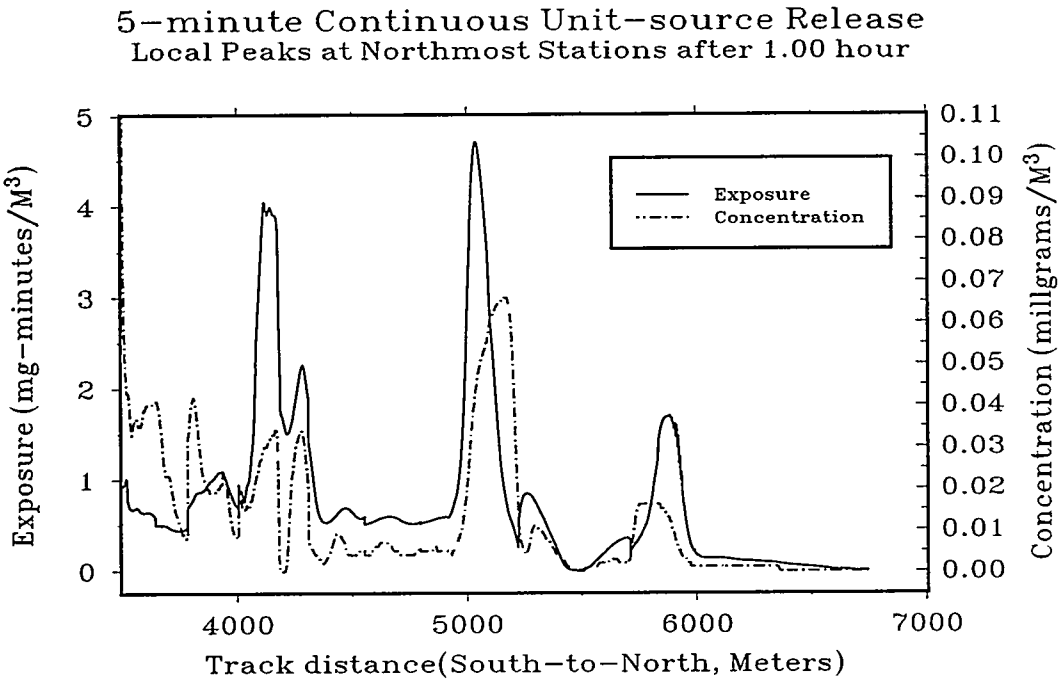

Figure 9: Local Concentration Peaks at Station Stops

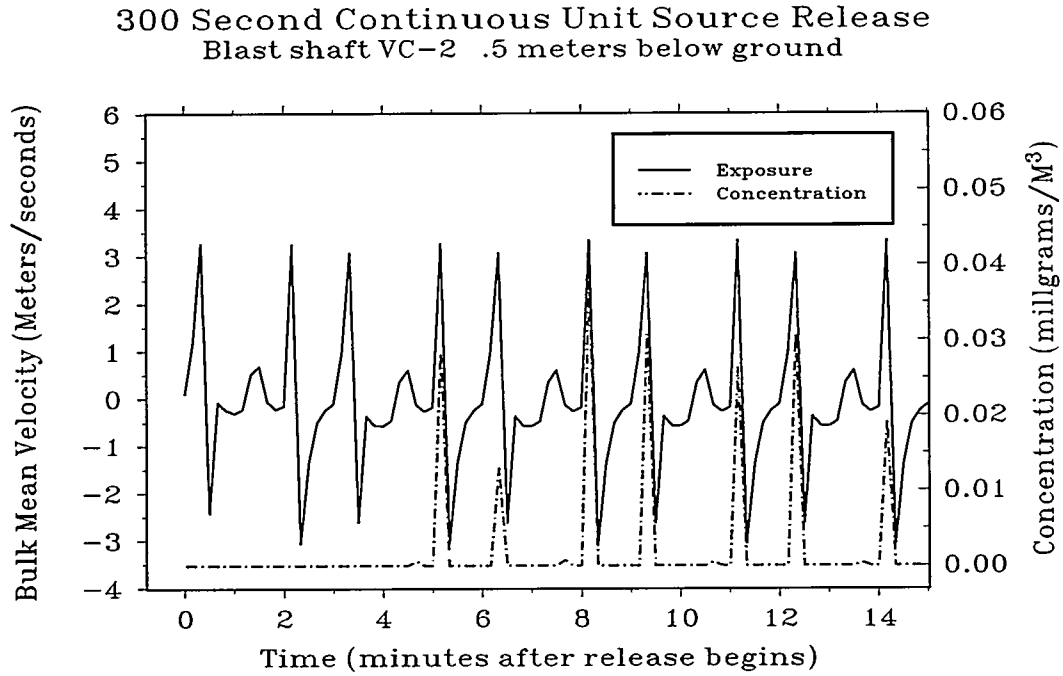

Figure 10: Velocity and Concentration at Ventilation Shaft Exit

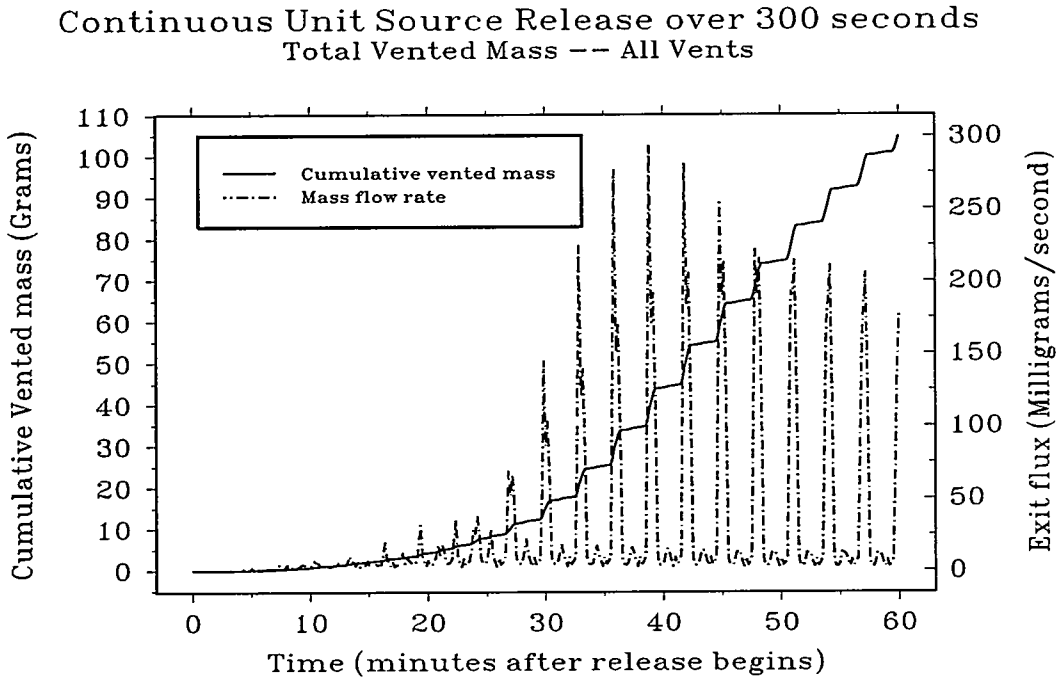

Figure 11: Flux & Cumulative Contaminant Mass Expelled from Relief Shaft

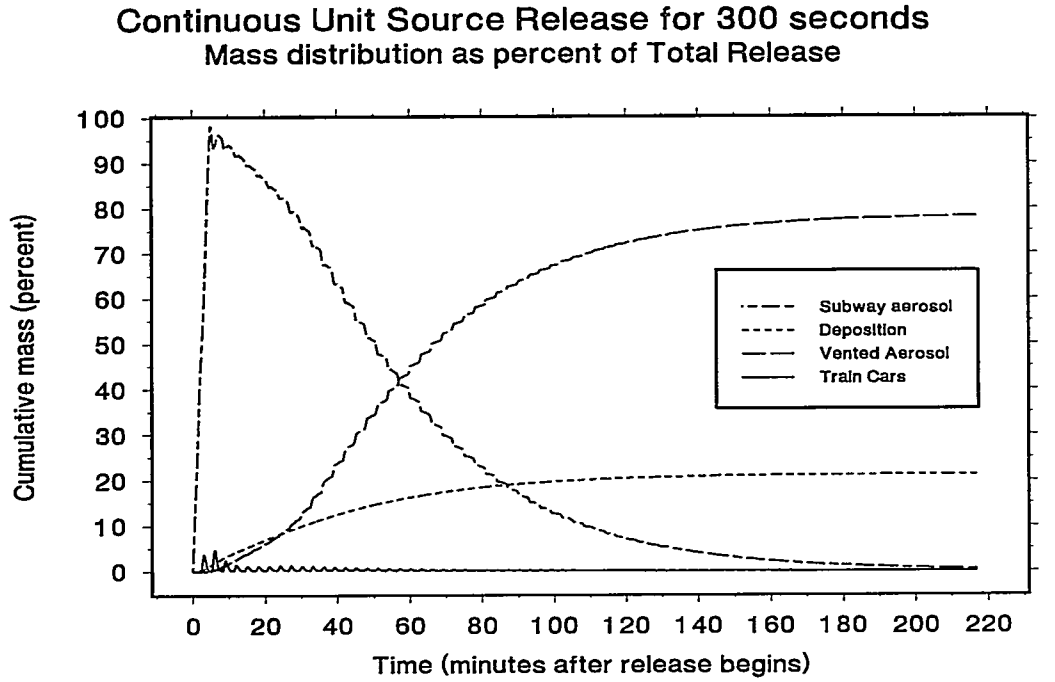

Figure 12: Cumulative Contaminant Mass Distribution